Journal of Alloys and Compounds 509 (2011) 4235–4241

Contents lists available at ScienceDirect

Journal of Alloys and Compounds

journal homepage: www.elsevier.com/locate/jallcom

Improvement of the electrochemical performance of $LiMn_2O_4$ cathode active material by lithium borosilicate (LBS) surface coating for lithium-ion batteries

Halil Şahan*, Hüseyin Göktepe, Şaban Patat, Ahmet Ülgen

Department of Chemistry, Faculty of Science, Erciyes University, Talas St., 38039 Kayseri, Turkey

ARTICLE INFO

Article history:
Received 30 August 2010
Received in revised form
31 December 2010
Accepted 9 January 2011
Available online 14 January 2011

Keywords:
Electrode materials
Coating materials
Chemical synthesis
Electrochemical reactions
X-ray diffraction
Scanning electron microscopy (SEM)

ABSTRACT

The LBS coating on the surface of spinel $LiMn_2O_4$ powder was carried out using the solid-state method, followed by heating at 425 °C for 5 h in air. The powder X-ray diffraction pattern of the LBS-coated spinel $LiMn_2O_4$ showed that the LBS coating medium was not incorporated in the spinel bulk structure. The SEM result showed that the LBS coating particles were homogeneously distributed on the surface of the $LiMn_2O_4$ powder particles. The effect of the lithium borosilicate (LBS) coating on the charge–discharge cycling performance of spinel powder ($LiMn_2O_4$) was studied in the range of 3.5–4.5 V at 1*C*. The electrochemical results showed that LBS-coated spinel exhibited a more stable cycle performance than bare spinel. The capacity retention of LBS-coated spinel was more than 93.3% after 70 cycles at room temperature, which was maintained at 71.6% after 70 cycles at 55 °C. The improvement of electrochemical performance may be attributed to suppression of Mn^{2+} dissolution into the electrolyte via the LBS glass layer.

1. Introduction

In recent years, $LiMn_2O_4$ spinel has been recognized as a promising cathode material for lithium-ion batteries because of its properties of high voltage, natural abundance, low cost and environmental benignity [1–3]. However, $LiMn_2O_4$ exhibits serious capacity fading during charge and discharge. The reason for capacity fading is attributed to several factors such as (i) Jahn–Teller distortion due to Mn^{3+} ions [4], (ii) spinel dissolution into the electrolyte [5,6], (iii) electrolyte decomposition at high potential regions [7] and (iv) loss of crystallinity during cycling [8]. On the other hand, some researchers have insisted that the Jahn–Teller effect is not an important factor for the capacity losses of spinel oxide in 4 V, and that capacity loss is caused by the simple dissolution of Mn^{3+} [9,10]. Myung et al. [11] reported that capacity fading is not related to structural change during cycling.

In order to overcome this capacity fading problem, two kinds of methods can be employed. One way is to substitute mono-, di- or trivalent cations in $LiMn_2O_4$ to reduce the Mn^{3+} ions which cause disproportion reactions. The other method is to coat the $LiMn_2O_4$ particles with various protective layers. Some studies have shown that the substitution of Mn ions at 16d sites with ions with a valence ≤+3 gives doped spinels $Li_xM_yMn_{2-y}O_4$ (M = Li, Mg, Zn, Al, Ni, Fe, Cr and Co), which could enhance cycling stability at room temperature [12–19]. Although this approach improves structural stability, it seriously reduces initial capacity, depending on the kind of substituted metals (M) and their content. Many research groups have also endeavoured to improve the poor capacity retention of the spinel material with anion substitution into the spinel structure [20,3].

Recently, surface modifications with oxides such as Li_2O–B_2O_3 [21,22], Al_2O_3 [23], Al_2O_3/CuO_x [24], ZnO [25,26], TiO_2 [27,28], $AlPO_4$ [29,30], CeO_2 [31], $LiAlO_2$ [32], SiO_2 [33], ZrO_2 [34] and Co_3O_4 [35] have been studied and have shown excellent cyclability. These studies considered that the presence of oxide coating can minimize the contact area of the $LiMn_2O_4$/electrolyte interface and suppress the dissolution of manganese.

Lithium-based superionic conducting glasses are found to exhibit higher ionic conductivity than their crystalline counterparts, since these glasses possess a more open structure for ionic transport. In addition, glassy superionic conductors can be prepared in varied compositions with high structural flexibility, homogeneity and chemical durability [36]. Thus, it is essential to study the effect of LBS glass coating on the cyclability of $LiMn_2O_4$. To the best of our knowledge, this is first time that such coating has been attempted as a means to improve the electrochemical performance of $LiMn_2O_4$ cathode material.

In this study, we report the preparation of LBS-coated spinel using the solid-state method and the effect of coating material on the electrochemical cycling performance of $LiMn_2O_4$. The treatment was expected to affect the cyclability. The preparation,

* Corresponding author. Tel.: +90 352 4374901x33185; fax: +90 352 4374933.
E-mail address: halil@erciyes.edu.tr (H. Şahan).

0925-8388/$ – see front matter © 2011 Elsevier B.V. All rights reserved.
doi:10.1016/j.jallcom.2011.01.054

structure and electrochemical performance of the surface-treated $LiMn_2O_4$ cathode material are discussed in comparison with the untreated one.

2. Experimental

Untreated $LiMn_2O_4$ was prepared by a glycine–nitrate combustion process [37]. Firstly, stoichiometric amounts of $LiNO_3$ (Riedel-de Haen) and $Mn(CH_3COO)_2{\cdot}4H_2O$ (Sigma) were dissolved in distilled water. Glycine (Merck) was added to the solution either as a solid or as a water solution. Its role was to serve both as a fuel for combustion and as a complexant to prevent inhomogeneous precipitation of individual components prior to combustion. Finally, nitric acid with the same mole of acetate anions was added to the solution. The molar ratio of glycine to nitrate was 1:4. The solution was heated continuously without any previous thermal dehydration. Afterwards the solution became a transparent viscous gel which auto-ignited, giving a voluminous, black, sponge-like ash product of combustion. The resulting ash was heated at 800 °C for 12 h.

In order to coat $LiMn_2O_4$ with LBS, xerogels of lithium borosilicate (LBS) were prepared by the sol–gel process using precursors of analar grade tetraethylorthosilicate ($Si(C_2H_5O)_4$, TEOS) (Merck), boric acid (Panreac) and lithium nitrate (Riedel-de Haen). The precursors were mixed according to their calculated molecular weight percentage under 2.5 N nitric acid concentration as a catalyst, using the following chemical composition:

$$20\%Li_2O - 80\%[0.2B_2O_3 + 0.8SiO_2](LBS)$$

The above composition and synthesis of LBS samples was fixed by Muralidharan in earlier studies [38]. The solutions of A–C were prepared separately by mixing the appropriate quantities of precursors to obtain the LBS compound. Calculated amounts of ethanol, water and TEOS were mixed in a 250 ml conical flask with a magnetic pellet, the mixture was found to be turbid initially but on stirring a clear solution was obtained. The water:TEOS ratio was maintained at 16:1 to form solution A. Solution B, containing boric acid in ethanol, was added to solution A with continual stirring and $x = 2.5$ N nitric acid was also added as an acid catalyst to the above mixture (A + B). The mixture of solution A and B was stirred for half an hour and later solution C, lithium nitrate in water, was added and stirred continuously at room temperature (RT) for about an hour. The temperature of the mixed solution was raised to 338 K and maintained for about 3 h with continual stirring. The sol was cast into plastic beakers covered with aluminium foil and maintained at 338 K in the oven. Aging of the gel was maintained at the same temperature (338 K) and resulted in transparent/opaque dried gels.

The mixture of the precursor gels of LBS glass with $LiMn_2O_4$ powders was thoroughly mixed with mortar and pestle, and the mixed powders were then calcined at 425 °C for 5 h. The weight ratio of the precursor of LBS glass to the $LiMn_2O_4$ powders for this method was 2 wt.%.

The cation composition of the base and surface-treated $LiMn_2O_4$ powders was determined by a flame atomic absorption spectrometer (AAS, Perkin Elmer 3110) and flame photometer (FP, Jenway PFP7) after dissolving the powders in a solution of 0.1 M 10 ml sulfuric acid of 0.1 M oxalic acid.

The phase identification and evaluation of the lattice parameters of the base and surface-treated $LiMn_2O_4$ powders were carried out by powder X-ray diffraction (XRD) using Cu Kα radiation (Bruker AXS D8). The diffractometer was equipped with a diffracted beam graphite monochromator. The diffraction data were collected at 40 kV and 40 mA over a 2θ range from 10° to 70° with a step size of 0.02° and a count time of 10 s per step. The DiffracPlus and Win-Metric programs were used to obtain the lattice parameters of the powders.

The particle morphology of the powders was examined by means of scanning electron microscopy (LEO 440), operated at 20 kV. Thermogravimetry (TG) and differential thermal analysis (DTA) measurements were conducted by the Perkin-Elmer (Diamond) high temperature thermal analyzer with 5–20 mg samples and a heating rate of 10 °C/min from 50 to 700 °C in air.

The electrochemical studies were carried out in two-electrode Teflon cells. The cells were fabricated by using the bare and surface-treated $LiMn_2O_4$ as a cathode and lithium foil as an anode. A glass fiber separator soaked in electrolyte separated the two electrodes. The electrolyte consisted of 1 M solution of $LiPF_6$ dissolved in ethylene carbonate (Aldrich)/diethyl carbonate (Merck) (EC/DEC, 1:1 ratio by volume). For the preparation of the cathode composite, a slurry mixed with 86 wt.% of cathode active material, 9 wt.% of acetylene black conductor (Alfa Aesar) and 5 wt.% of polyvinylidene fluoride (PVDF, Fluka) binder in 1-methyl-2-pyrrolidone (NMP, Merck) was pasted on the aluminium foil current collector with a diameter of 13 mm, followed by vacuum drying at 120 °C overnight in a vacuum oven and uniaxial pressing between two flat plates at 2 tons for 5 min. The electrode loading consisted of about 4 mg of cathode active material. Diethyl carbonate, ethylene carbonate, and acetylene black were used after being purified according to the methods given in the literature [39]. *Diethyl carbonate*: 100 ml DEC was washed with an aqueous 10% Na_2CO_3 (20 ml) solution, saturated $CaCl_2$ (20 ml), then water (30 ml). After drying by standing over solid $CaCl_2$ for 1 h (note that prolonged contact should be avoided because slow combination with $CaCl_2$ occurs), it was fractionally distilled. *Ethylene carbonate*: This was dried over P_2O_5 then fractionally distilled at 10 mm Hg pressure and crystallized from dry ethyl ether respectively. *Acetylene black*: It was leached for 24 h with 1:1 HCl to remove oil contamination, then washed repeatedly with distilled water. It was then dried in air, and eluted for one day each with benzene and acetone. It was again dried in air at room temperature, then heated in a vacuum for 24 h at 600 °C to remove adsorbed gases.

Charge–discharge tests were performed galvanostatically at a current rate of 1*C* with cut-off voltages of 3.5–4.5 V (vs Li/Li^+) at room and elevated temperature (25 °C and 55 °C). The potential scan rate was 100 μV/s in the cyclic voltammogram (CV) experiment between 3.0 and 4.4 V. All electrochemical experiments were performed using a multi-channel battery tester (PAR, VersaSTAT MC Multichannel Potentiostat/Galvanostat). All processes of assembling and dismantling the cells were carried out in an argon-filled dry glove box.

In order to verify the effect of the LBS-coated layer on reducing the dissolution of spinel $LiMn_2O_4$, a Mn dissolution experiment was also carried out in this study. Bare and LBS-coated $LiMn_2O_4$ powders were immersed in an electrolyte solution consisting of 1 M $LiPF_6$ in 1:1 mixture by volume of EC/DEC at room temperature. The weight of immersed cathode powders was 0.01 g, and the volume of the electrolyte was 3 ml. After immersing the powders at 3 days, the resulting electrolytes were filtered. A 0.5 ml part of electrolytes was diluted with 0.1 N HNO_3 and analyzed via ICP-MS (Agilent 7500-a) to determine the concentrations of the dissolved Mn^{2+} ions.

3. Results and discussion

3.1. Crystal structure and surface morphology

The chemical analysis of the bare and surface-treated lithium manganese oxide indicated that the stoichiometry of the elements was very close to the targeted formula.

To determine the effect of LBS coating on the crystal structure of $LiMn_2O_4$, X-ray powder diffraction was carried out on uncoated and coated spinel materials. The XRD patterns of the bare and LBS-coated $LiMn_2O_4$ samples are presented in Fig. 1. Because the LBS phase was amorphous, the presence of LBS in the sample was not detected by XRD. The XRD data shows that bare and LBS-coated $LiMn_2O_4$ (Fig. 1b and c) were identified as well-defined single-phase products with a cubic spinel structure in the Fd3m with space group. There is no significant change in the XRD pattern for the coated spinel material in Fig. 1c, compared with the bare one. Lattice parameters calculated by the Win-Metric program were $a = 8.237$ Å and $a = 8.236$ Å, respectively for the base and LBS-coated materials. Almost no change in the lattice parameter for both samples indicated that the LBS coating medium was not incorporated into the spinel structure but only presented on the surface of $LiMn_2O_4$, since Li^+, B^{3+} and Si^{4+} introduction into the spinel structure leads to significant change in the lattice parameter. If Li^+, B^{3+} and Si^{4+} ions were substituted for Mn^{3+} ions in the crystal lattice, the lattice parameter of the substituted spinel would be smaller than that of undoped spinel $LiMn_2O_4$. This is due to the smaller size of Li^+ (0.59 Å), B^{3+} (0.27 Å) and Si^{4+} (0.40 Å) as compared with the larger Mn^{3+} (0.66 Å) [40].

To work out the possible chemical composition of the coating layer, a thermal gravimetric examination of the precursor powder of the coating material, obtained from the evaporation of the LBS xerogel solution, was carried out and the results can be seen in Fig. 2. There is a drastic weight loss to 100 °C is seen due to the evaporation of absorbed water from the precursor. Then, a minor decrease in weight is seen between 115 °C and 200 °C, which is attributed to the decomposition of nitrates. Decomposition of the organic phase is also seen between 200 °C and 485 °C. No obvious change is observed above 500 °C. As can be seen from Fig. 1a calcination of the precursor powder at 425 °C for 5 h exhibited an amorphous LBS. Therefore, it is believed that the spinel shown in Fig. 1c is coated with LBS.

The surface morphology change of $LiMn_2O_4$ after coating with LBS is presented in Fig. 3. It is seen that the particle size of uncoated-$LiMn_2O_4$ particles is about 200 nm, and there is no size difference between the bare and the LBS-modified $LiMn_2O_4$ particles. On the other hand, the surface morphology of the uncoated $LiMn_2O_4$ particles is smooth, as shown in Fig. 3a, but it becomes aggregated after coating with LBS (Fig. 3b).

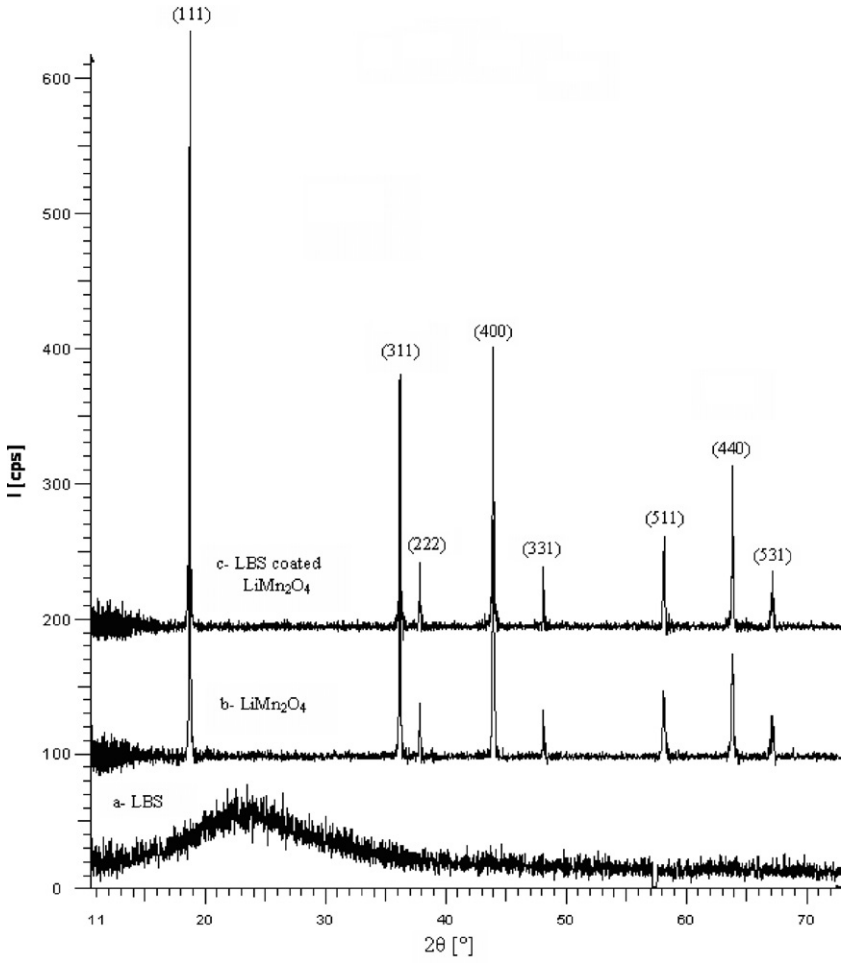

Fig. 1. X-ray diffraction patterns of (a) LBS glass produced from calcination of the precursor powder of coating material, (b) bare $LiMn_2O_4$ and (c) LBS-coated $LiMn_2O_4$.

Fig. 4 shows the electron probe micro-analysis results obtained on LBS-coated spinel powder. As can be seen in the image, it was found that the distribution of silicon on the powder surface is fairly uniform. As a result, it can be confirmed that the surface of $LiMn_2O_4$ was successfully coated with LBS particles.

3.2. Electrochemical properties

Fig. 5 shows the continuous charge and discharge profiles of the bare and surface-treated $LiMn_2O_4$ by applying a current of 148 mA g^{-1} (1*C*-rate) for the potential range 3.5–4.5 V (vs Li/Li^+) at

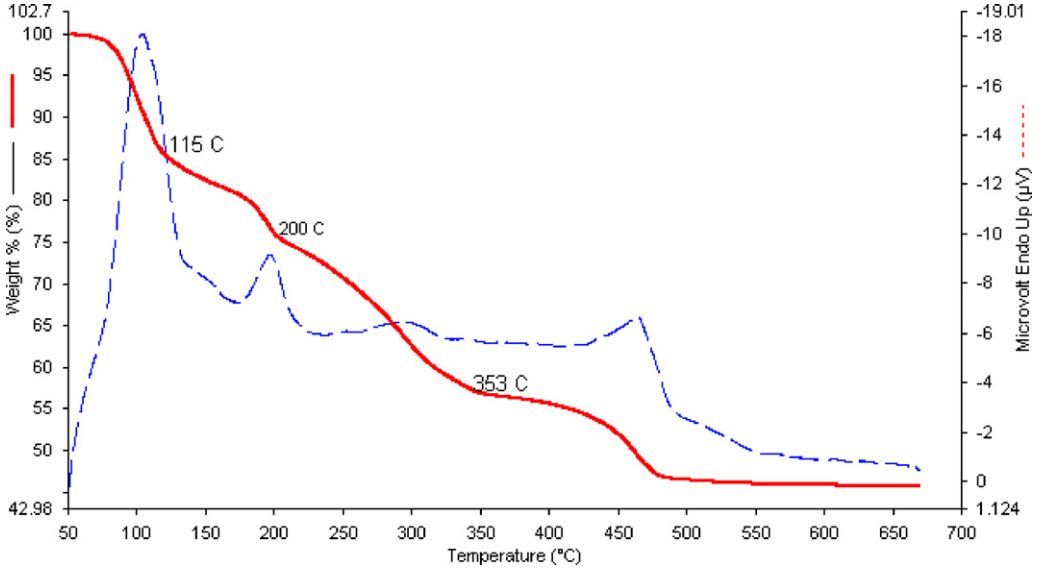

Fig. 2. Thermal-gravimetric curve of LBS precursor powder as the coating medium obtained from evaporation of solution.

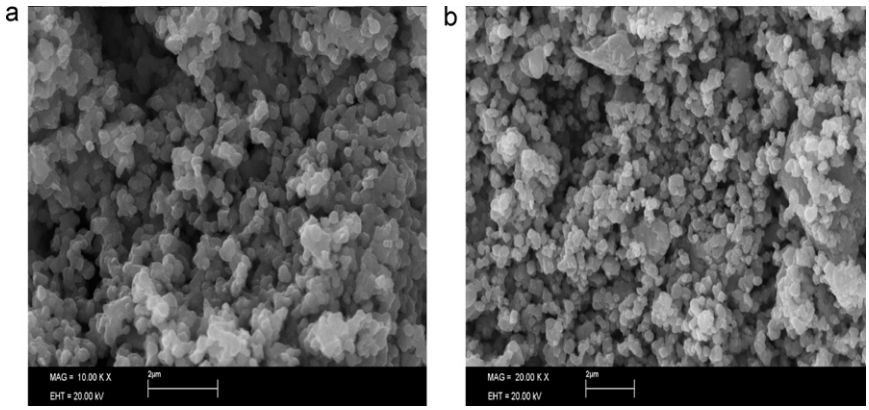

Fig. 3. SEM images of (a) bare $LiMn_2O_4$, (b) LBS-coated $LiMn_2O_4$.

room temperature. It can be clearly seen that the charge/discharge curves of all the samples have two voltage plateaus at approximately 4.1 and 4.0 V, originating from the $Mn^{3+/4+}$ redox couple, which indicated a remarkably well-defined $LiMn_2O_4$ spinel. Two voltage plateaus indicate that the insertion and extraction of lithium ions occur in two stages [41]. The first plateau at 4.0 V is associated with the single-phase reversible reaction of $LiMn_2O_4 \rightarrow Li_{0.5}Mn_2O_4 + 0.5\ Li^+$, while the second one at 4.1 V is attributed to the two-phase reaction of $Li_{0.5}Mn_2O_4 \rightarrow Mn_2O_4 + 0.5\ Li^+$. As can be seen in Fig. 5, the two potential plateaus for both samples were maintained after the 70th cycle.

The typical cyclic voltammograms of bare $LiMn_2O_4$ and LBS-coated $LiMn_2O_4$ electrodes were carried out using pure lithium foil acting as a counter and reference electrode in the potential range between 3.0 and 4.4 V at a scan rate of 100 μV/s. Two cells were freshly cycled and were then used for testing the galvanostatic charge/discharge studies at room temperature. After the completion of the 50th cycle the two cells were again characterized by the cyclic voltammogram. The cyclic voltammogram showed two couples of redox peaks at around 4.02 and 4.15 V. The split of redox peaks into two couples indicates that the electrochemical intercalation and de-intercalation reactions of lithium ion proceed in two steps. As shown in Fig. 6b, the CV peaks related to the LBS-coated $LiMn_2O_4$ electrode are much more steady compared to the peaks of the bare electrode. These differences indicate that the LBS-coated $LiMn_2O_4$ electrode has better reversibility than that of the bare spinel electrode.

Fig. 7 represents the cycling performances of bare and LBS-coated $LiMn_2O_4$ cathode material for rechargeable lithium-ion batteries. Li/$LiMn_2O_4$ and Li/LBS-coated $LiMn_2O_4$ cells were characterized by all charge/discharge cycling at a current rate of 1*C* in the potential region between 3.5 and 4.5 V at room temperature (25 °C). The discharge capacity and capacity fading rates for different numbers of cycles are evaluated and presented in Table 1. From the figure, we can see that the surface-modified $LiMn_2O_4$ cathode material displays a lower discharge capacity (109.7 mAh g^{-1}) than the bare one. This can be explained by the fact that the LBS layer forms a barrier to the movement of Li ions, which hinders the extraction and insertion of Li ions from the spinel and results in the low initial specific capacity of the cathode [42]. As seen in Table 1 and Fig. 6, after 70 cycles between 3.5 and 4.5 V at a 1*C* charge–discharge rate, the discharge capacity of the bare $LiMn_2O_4$ faded from 115.3 to 86.0 mAh g^{-1} with the retention of 74.6% of its initial capacity. However, under the same condi-

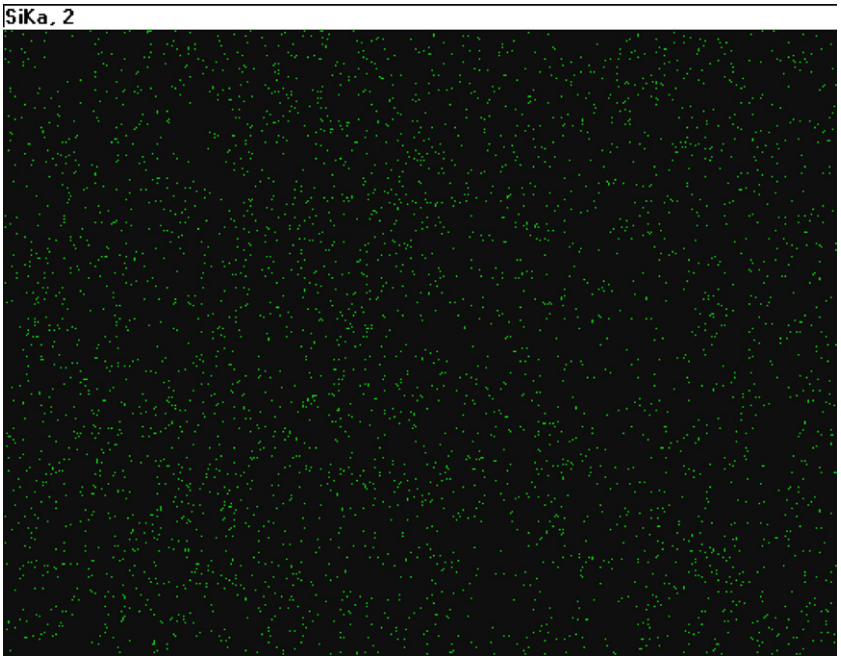

Fig. 4. Electron probe micro-analysis image of Si element for LBS-coated spinel.

Table 1
Discharge capacity performance of bare $LiMn_2O_4$ and surface-treated $LiMn_2O_4$ cells[a].

Cathode materials	Discharge capacity (mAh g^{-1})							Capacity retention (%)
	1st	5th	10th	30th	50th	60th	70th	
$LiMn_2O_4$								
25 °C	115.3	106.2	101.3	93.0	89.3	89.0	86.0	74.6
55 °C	104.2	92.3	82.4	68.5	61.1	58.3	55.4	53.2
LBS coated $LiMn_2O_4$								
25 °C	108.9	109.7	108.5	106.4	103.9	103.5	102.3	93.3
55 °C	120	111.4	107.7	96.9	90.4	88.4	85.9	71.6

[a] Loss of discharge capacity at the last cycle is compared with that at maximum discharge capacity.

tions, the discharge capacity of the LBS-coated spinel electrodes clearly shows an improved cycling behavior compared with the bare one. The LBS-coated $LiMn_2O_4$ exhibits maximum discharge capacity of 109.7 mAh g^{-1}, but after 70 cycles 93.3% capacity retention was obtained and the discharge capacity was still maintained at 102.3 mAh g^{-1}. This cycling behavior of the LBS-coated $LiMn_2O_4$ indicates that LBS coating significantly improved cycling performances at room temperature. As mentioned in other papers, surface coating of $LiMn_2O_4$ by some stable substances, e.g. TiO_2 [27], $AlPO_4$ [30], CeO_2 [31], SiO_2 [33], amphoteric oxides [43], and Cr_2O_3 [44], enhanced the cycling behavior of the spinel cathode at room temperature. As shown in the literature, the capacity retention of SiO_2, amphoteric oxides and $AlPO_4$ coated cathodes were obtained 96.6%, 95.8% and 96.5% after 70 cycles at 0.5*C* rate, respectively. In addition, the capacity retention of CeO_2, Cr_2O_3 and TiO_2 coated cathodes were obtained 92.3%, 94.4%, and 82.5% after 70 cycles at 1*C* rate respectively.

The changes of morphology after cell tests are given in Fig. 8. As shown in the figures, the SEM micrographs of the bare $LiMn_2O_4$ electrode after 70 cycles at room temperature (Fig. 8b) were different from those of the LBS-coated $LiMn_2O_4$ electrode (Fig. 8d). The LBS-coated $LiMn_2O_4$ electrode preserved its original surface morphology, while physical destruction on the surface of the bare $LiMn_2O_4$ electrode was observed. Abnormal surfaces which formed on the bare spinel after the cell test may be a by-product of the decomposition of the electrolyte [24].

The ICP analysis results for the bare and the LBS-coated $LiMn_2O_4$ spinels dissolution into the electrolyte were found to be 26.76 ppm and 13.68 ppm Mn, respectively. These results indicated that the LBS coating on the spinel $LiMn_2O_4$ particles could suppress the dissolution of manganese ions into the electrolyte and clearly improve the cyclability of the spinel $LiMn_2O_4$ cathode materials.

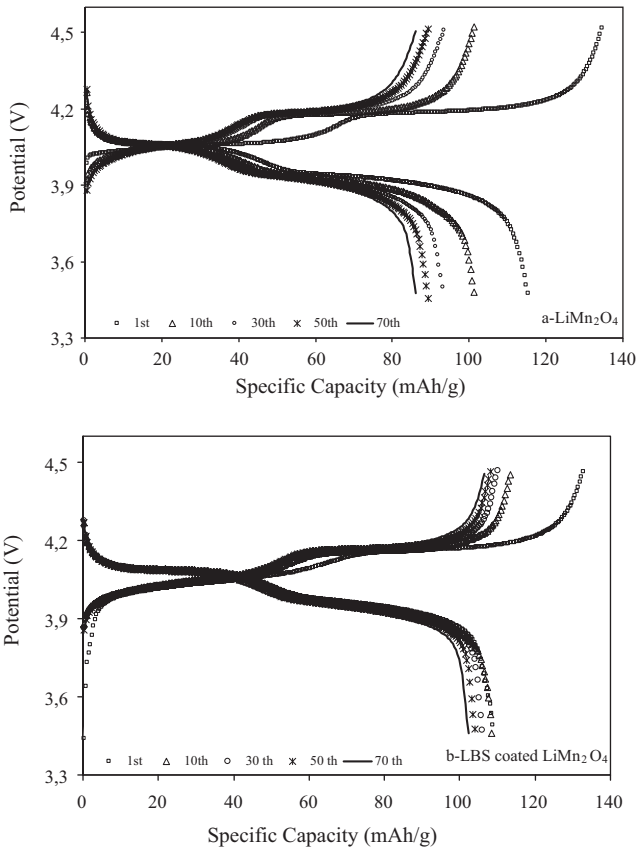

Fig. 5. Continuous charge–discharge curves during 70 cycles: (a) bare $LiMn_2O_4$ and (b) LBS-coated $LiMn_2O_4$. The applied current density is 148 mA g^{-1} (1*C*-rate) at room temperature. Li metal was used as the anode.

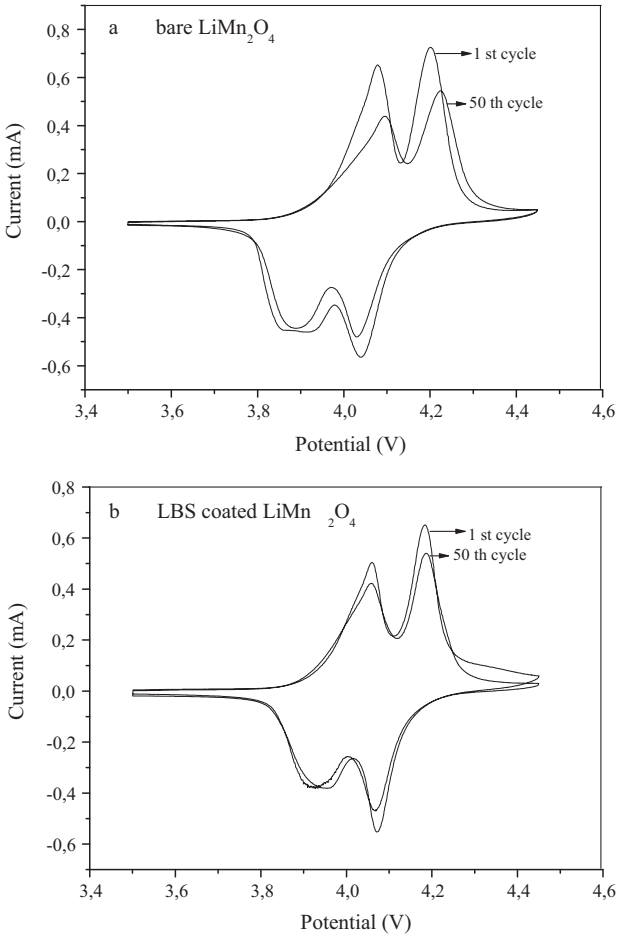

Fig. 6. Typical cyclic voltammetric curves of initial and 50th cycle for (a) $LiMn_2O_4$ and (b) LBS-coated $LiMn_2O_4$ cycled between 3.0 and 4.5 V at scan rate of 100 μV/s.

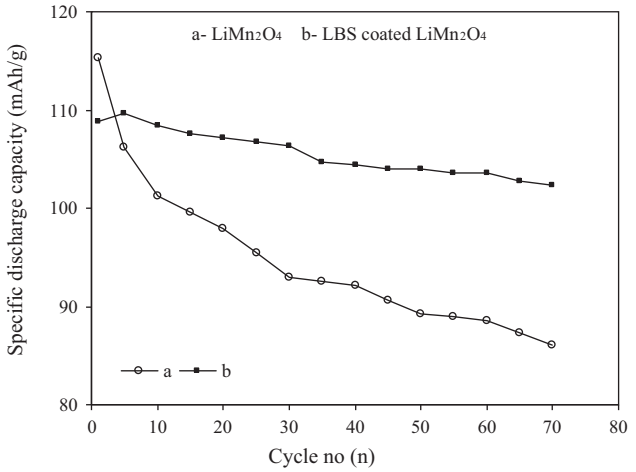

Fig. 7. Cycling performances of (a) the bare $LiMn_2O_4$ and (b) LBS-coated $LiMn_2O_4$ at a current level of 1*C* (148 mA g^{-1}) in the voltage range of 3.5–4.5 V at room temperature.

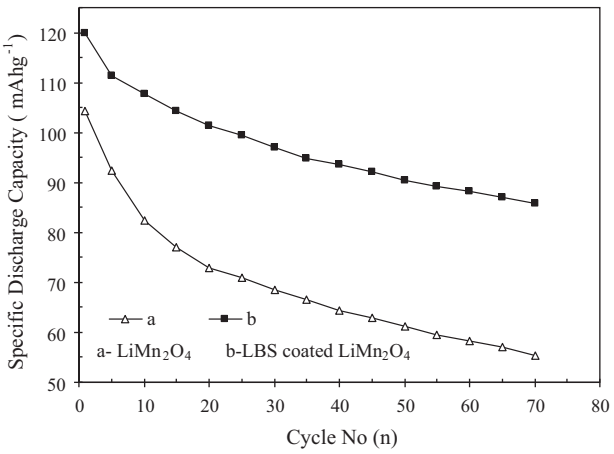

Fig. 9. Discharge capacities of bare and LBS-coated $LiMn_2O_4$ cathodes in the range of 3.5–4.5 V with a constant current density of 1*C* at 55 °C.

The electrochemical cycling performance of the bare and LBS-coated $LiMn_2O_4$ cathodes at elevated temperature (55 °C) are shown in Fig. 9. As seen from Fig. 9 and Table 1, after 70 cycles between 3.5 and 4.5 V at 1*C* charge–discharge rate, the discharge capacity of the bare $LiMn_2O_4$ faded from 104.2 to 55.4 mAh g^{-1} with the retention of 53.2% of its initial capacity. However, under the same conditions, the discharge capacity of the LBS-coated spinel electrodes clearly shows an improved cycling behavior compared with the bare one. After 70 cycles between 3.5 and 4.5 V at 1*C* charge–discharge rate, the discharge capacity of the LBS-coated $LiMn_2O_4$ faded from 120 to 85.9 mAh g^{-1} with the retention of 71.6% of its initial capacity. Therefore, it is proposed that LBS coating is an effective way of improving the elevated temperature capacity retention of $LiMn_2O_4$.

As Xia et al. [10] reported, capacity loss caused by dissolution of manganese accounted for 23% of overall capacity loss at room temperature. Jang et al. [9] confirmed that HF, generated during cycling when using $LiPF_6$-based electrolyte, was responsible for the dissolution of manganese. In fact, preparation of H_2O-free electrolyte containing $LiPF_6$ in organic solvent is difficult. A small amount of water (though the amount is less than 20 ppm) facilitates the decomposition of electrolytic salt, $LiPF_6$. Thus, HF is formed as a by-product by the following reaction [45].

$$LiPF_6 + H_2O \rightarrow LiF + POF_3 + 2HF$$

The generated acid, HF, continuously attacks the active material and this decomposes as the cycle progresses, causing capacity fading

$$2LiMn_2O_4 + 4H^+ \rightarrow 3\lambda\text{-}MnO_2 + Mn^{2+} + 2Li^+ + 2H_2O$$

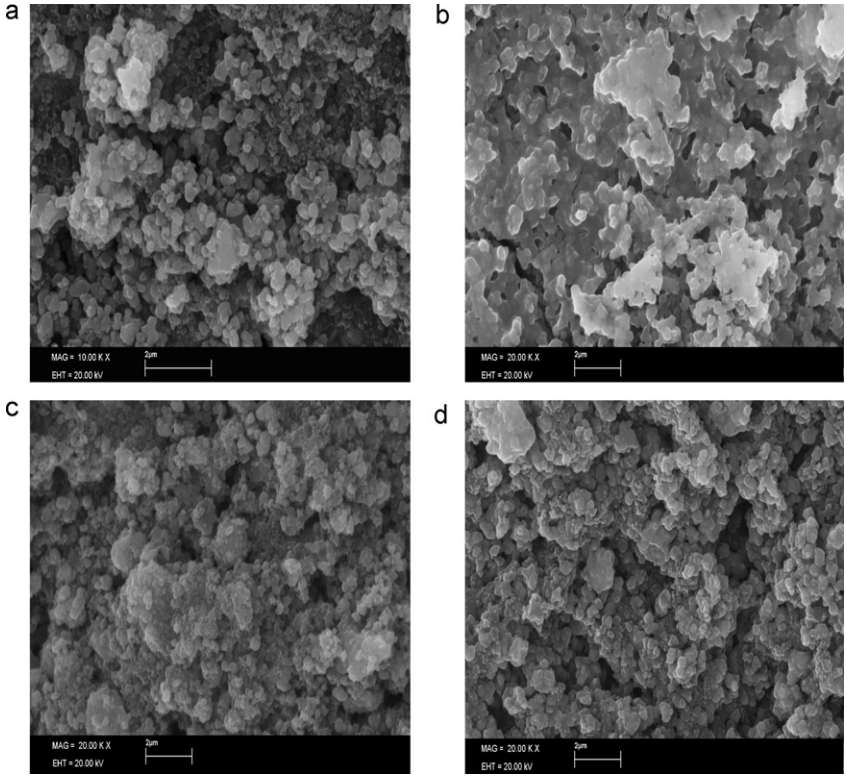

Fig. 8. SEM micrographs of bare $LiMn_2O_4$ (a) as prepared, (b) after 70 cycles at RT and LBS-coated $LiMn_2O_4$ (c) as prepared, and (d) after 70 cycles at RT.

Therefore, it is possible that Mn dissolution could be reduced by decreasing HF content at the cathode surface. The electrochemical data obtained in this study demonstrated that the cycling performance of the $LiMn_2O_4$ spinel electrode was significantly improved by surface coating of LBS. The LBS coating prevented direct contact between the spinel and the electrolyte and therefore reduced the dissolution of manganese and the oxidation of electrolyte.

Coating the spinel $LiMn_2O_4$ with a LBS glass layer resulted in a tremendous improvement in retention capacity at room and elevated temperatures.

4. Conclusions

The $LiMn_2O_4$ cathode was successfully coated with LBS using tetraethylorthosilicate, boric acid and lithium nitrate as the precursor. The LBS coating did not result in a change in the host structure of $LiMn_2O_4$. The LBS glasses were uniformly dispersed on the surface of spinel $LiMn_2O_4$ particles. The discharge capacity of the LBS-coated spinel electrodes showed an improved cycling behavior compared with the bare one. The improved performance of the surface-treated sample was ascribed to the LBS coating on the surface of the $LiMn_2O_4$ material, which prevented direct contact between the $LiMn_2O_4$ particles and electrolyte, and therefore reduced the dissolution of manganese and the oxidation of electrolyte. The capacity retention of the LBS-coated $LiMn_2O_4$ over 70 cycles was 93.3% and 71.6%, while the untreated one showed 74.6% and 53% capacity retention of the initial discharge capacity at room and elevated temperature, respectively. Therefore, LBS coating is an effective way to improve the electrochemical performance of $LiMn_2O_4$ cathode material.

Acknowledgements

This study was financially supported by the Kayseri Governorship's Middle Anatolian Development Agency and the Research Foundation of Erciyes University (FBA-08-439). The authors would like to thank Mr. I. Akşit and Mrs. F. Kılıç for the SEM observation.

References

[1] M.M. Thackeray, W.I.F. David, P.G. Bruce, J.B. Goodenough, Mater. Res. Bull. 18 (1983) 461–472.
[2] D. Guyomard, J.M. Tarascon, J. Electrochem. Soc. 139 (1992) 937–948.
[3] S.H. Park, K.S. Park, Y.K. Sun, K.S. Nahm, J. Electrochem. Soc. 147 (2000) 2116–2121.
[4] A. Yamada, M. Tanaka, K. Tanaka, K. Sekai, J. Power Sources 81–82 (1999) 73–78.
[5] D.H. Jang, S.M. Oh, Electrochim. Acta 43 (1998) 1023–1029.
[6] T. Aoshima, K. Okahara, C. Kiyohara, K. Shizuka, J. Power Sources 97–98 (2001) 377–380.
[7] Y. Gao, J.R. Dahn, Solid State Ionics 84 (1996) 33–40.
[8] Y. Shao-horn, S.A. Hackney, A.J. Kahaian, K.D. Kepler, E. Skinner, J.T. Vaughey, et al., J. Power Sources 81–82 (1999) 496–499.
[9] D.H. Jang, Y.J. Shin, S.M. Oh, J. Electrochem. Soc. 143 (1996) 2204–2211.
[10] Y. Xia, Y. Zhou, M. Yoshio, J. Electrochem. Soc. 144 (1997) 2593–2600.
[11] S.T. Myung, H.T. Chung, S. Komaba, N. Kumagai, H.B. Gu, J. Power Sources 90 (2000) 103–108.
[12] R.J. Gummow, A. de Kock, M.M. Thackeray, Solid State Ionics 69 (1994) 59–67.
[13] S.T. Myung, S. Komaba, N. Kumagai, J. Electrochem. Soc. 148 (2001) A482–489.
[14] K. Amine, H. Tukamoto, H. Yasuda, Y. Fujita, J. Power Sources 68 (1997) 604–608.
[15] B. Banov, Y. Todorov, A. Trifonova, A. Momchilov, V. Manev, J. Power Sources 68 (1997) 578–581.
[16] F. Bonino, S. Panero, D. Satolli, B. Scrosati, J. Power Sources 97–98 (2001) 389–392.
[17] L. Hernan, J. Morales, L. Sanchez, J. Santos, Solid State Ionics 118 (1999) 179–185.
[18] H. Şahan, H. Göktepe, Ş. Patat, Inorg. Mater. 44 (2008) 420–425.
[19] H. Göktepe, H. Şahan, Ş. Patat, A. Ülgen, Ionics 15 (2009) 233–239.
[20] Y.K. Sun, Y.S. Jeon, H.J. Lee, Electrochem. Solid-State Lett. 3 (2000) 7.
[21] G.G. Amatucci, A. Blyr, C. Sigala, P. Alfonse, J.M. Tarascon, Solid State Ionics 104 (1997) 13–25.
[22] H. Şahan, H. Göktepe, Ş. Patat, A. Ülgen, Solid State Ionics 178 (2008) 1837–1842.
[23] S.W. Lee, K.S. Kim, H.S. Moon, H.J. Kim, B.W. Cho, W.I. Cho, et al., J. Power Sources 126 (2004) 150–155.
[24] S.W. Lee, K.S. Kim, K.L. Lee, H.S. Moon, H.J. Kim, B.W. Cho, W. Cho, J.W. Park, J. Power Sources 130 (2004) 233–240.
[25] R. Alcantara, M. Jaraba, P. Larcla, J.L. Tirado, J. Electroanal. Chem. 566 (2004) 187–192.
[26] J. Tu, X.B. Zhao, J. Xie, G.S. Cao, D.G. Zhuang, T.J. Zhu, et al., J. Alloy Compd. 432 (2007) 313–317.
[27] L. Yu, X. Qiu, J. Xi, W. Zhu, L. Chen, Electrochim. Acta 51 (2006) 6406–6411.
[28] A. Eftekhari, J. Power Sources 130 (2004) 260–265.
[29] J. Cho, Y.W. Kim, B. Kim, J.G. Lee, B. Park, Angew. Chem., Int. Ed. 42 (2003) 1618–1621.
[30] D. Liu, Z. He, X. Liu, Mater. Lett. 61 (2007) 4703–4706.
[31] H.W. Ha, N.J. Yan, K. Kim, Electrochim. Acta 52 (2007) 3236–3241.
[32] Y.C. Sun, Z.X. Wang, L.Q. Chen, X.J. Huang, J. Electrochem. Soc. 150 (2003) A1294–1298.
[33] D. Arumugam, G.P. Kalaignan, J. Electroanal. Chem. 624 (2008) 197–204.
[34] S. Lim, J. Cho, Electrochem. Commun. 10 (2008) 1478–1481.
[35] K.S. Lee, S.T. Myung, H. Bang, K. Amine, D.W. Kim, Y.K. Sun, J. Power Sources 189 (2009) 494–498.
[36] E.A. Hayri, M. Greenblatt, J. Non-Cryst. Solids 94 (1987) 387–401.
[37] Y. Zhang, H.C. Shin, J. Dong, M. Liu, Solid State Ionics 171 (2004) 25–31.
[38] P. Muralidharan, M. Venkateswarlu, N. Satyanarayana, Mater. Chem. Phys. 88 (2004) 138–144.
[39] W.L.F. Armarego, D.D. Perrin, Purification of Laboratory Chemicals, fourth ed., Oxford, Butterworth/Heinemann, 2002.
[40] D.W. Green, R.H. Perry, Perry's Chemical Engineers' Handbook, eighth ed., McGraw-Hill, New York, 2008.
[41] C. Sigala, D. Guyomard, A. Verbaere, Y. Piffard, M. Tournoux, Solid State Ionics 81 (1995) 167–170.
[42] Y. Xia, M. Yoshio, J. Electrochem. Soc. 143 (3) (1996) 825–833.
[43] S.B. Park, H.C. Shin, W.G. Lee, W. Cho, H. Jang, J. Power Sources 180 (2008) 597–601.
[44] H. Şahan, H. Göktepe, Ş. Patat, A. Ülgen, Solid State Ionics 181 (2010) 1437–1444.
[45] S.T. Myung, K. Izumi, S. Komaba, Y.K. Sun, H. Yashiro, N. Kumagai, Chem. Mater. 17 (2005) 3695–3704.